JNCS Journal of Nepal Chemical Society July 2025, Vol. 45, No. 2, 64-74
ISSN: 2091-0304 (print)
DOI: https://doi.org/10.3126/jncs.v45i2.83036
RESEARCH ARTICLE

Shish-Kebab Nanohydroxyapatite-TiO_2 Nanofiber: A Biomimetic Platform for Regenerative Medicine

Shiva Pandeya[1, 2, 3], Shiv Kumar Sah[3], Ziliang Li[1*], Mahesh Kumar Joshi[1, 2*]

[1]*School of Materials Science and Engineering, Liaocheng University, Liaocheng 252059, China*

[2]*Central Department of Chemistry, Tribhuvan University, Kathmandu, Nepal*

[3]*Department of Pharmacy, Institute of Medicine, Tribhuvan University, Kathmandu, Nepal*

**Corresponding E-mail: mahesh.joshi@trc.tu.edu,*

(Received: May 20, 2025, revised: June 14, 2025 accepted: July 15, 2025)

Abstract

Flexible titanium dioxide (TiO_2) nanofibers are gaining considerable attention in bone tissue engineering owing to their superior biocompatibility, extensive surface area, and structural adaptability. This study explores the synthesis of flexible TiO_2 nanofibers and its in vitro evaluation for biomineralization capability. The Flexible TiO_2 NFM was fabricated employing electrospinning technique followed by controlled calcination. The SEM-EDS, TEM, XRD, and FTIR analysis were done to characterize and to confirm the biomineralization of the flexible TiO_2 NFM. Surface analysis via scanning electron microscopy (SEM) revealed the progressive formation of apatite-like layers. Elemental confirmation was provided by energy-dispersive X-ray spectroscopy (EDS), which identified the presence of calcium (Ca) and phosphorus (P), with Ca/P ratios nearing the ideal value for stoichiometric hydroxyapatite (~1.64). EDS spectra displayed characteristic peaks for oxygen at~0.52 keV, calcium at 3.69 keV & 4.01 keV, and phosphate 2.01 keV, confirming the deposition of calcium phosphate and the effectiveness of the biomineralization process. XRD analysis for biomineralized NFM showed distinct peaks at 2θ values of 28.5°, 31.7°, and 66.3°. Likewise FTIR analysis showed notable alterations with characteristics peaks at 3418 cm^{-1} suggesting increased hydrophilicity, and 1625.96 cm^{-1}, 1394.55 cm^{-1}, 1034.65 cm^{-1} for confirmation of calcium phosphate phase, such as hydroxyapatite. The presence of granular textures on the fiber surface indicated the successful formation of apatite-like structures. TEM analysis revealed a well-defined crystalline core surrounded by a biomineralized layer, closely resembling the mineral composition of natural bone. The results of XRD and FTIR peaks further confirmed the biomineralization of flexible TiO_2 NFM.

Keywords: Flexibility, Biomineralization, In vitro analysis, Hydroxyapatite, Bone integration

Introduction

The development of teeth, shells, bones, and some protective coatings is governed by biomineralization, which is the natural mineral created by living things to harden or stiffen the tissues. The field of biomineralization of fibers has been created in response to growing interest in understanding and using biomineralization to enhance fibrous materials, both biologically and synthetically [1]. Fibers give mechanical support and serve as scaffolds to direct the growth and arrangement of minerals, producing materials with .....

remarkable durability, strength, and flexibility [2]. To produce sophisticated fiber materials, these days' researchers use synthetic methods that imitate these natural processes [3]. Through the process of biomineralization, the mechanical characteristics, thermal stability, and biological functions of fibers can be improved. Modification on the mineral type, crystal size, and deposition patterns allows the fine-tuning of biomineralized fibers' characteristics, which is one of its main advantages [4]. Sustainability in the environment is yet another critical component. The biomineralization of fibers is a potent natural and artificial process that blends the durability and hardness of inorganic minerals with the strength and flexibility of organic fibers. Applications in materials science, environmental sustainability, and healthcare all have a lot of potential. Biomineralized fiber technologies will probably become more significant as our knowledge grows in the creation of smart materials and next-generation composites. Biomineralization usually consists of a number of important processes [5, 6]. The first step in attracting and nucleating minerals is to activate or functionalize the fiber surface. After that, the fiber surface interacts with supersaturated mineral ion solutions, including calcium, phosphate, or silica. The process of controlled nucleation and crystal growth results in the development of a mineralized layer that closely resembles the structure of the fiber.

Biomineralization on nanofibers is a fast developing field of study that combines the unique properties of nanomaterials with the inherent advantages of mineralized structures. Nanofibers' high surface area-to-volume ratio, mechanical strength, and flexibility make them ideal for mineral deposition [7]. These nanofibers gain new properties through the biomineralization process, which is crucial for a number of innovative uses, particularly in the fields of biology, the environment, and engineering. Biomineralized nanofibers have demonstrated potential in wound healing [8], regenerative medicine [9], tissue engineering [10], and environmental applications [11]. Biomineralization considerably improves the mechanical, thermal, and chemical stability of nanofibers from the standpoint of materials science [12]. Additionally, by permitting multifunctional qualities, biomineralization enhances the performance of nanofibers. Moreover, the technique itself is very sustainable and draws inspiration from nature. In summary, biomineralization of nanofibers is a potent technique that blends nanotechnology and biological inspiration to produce materials with exceptional functionality and performance.

Inorganic nanofibers significantly contribute to the advancement of biomineralization by offering robust, biocompatible, and adaptable scaffolds that direct the regulated creation of useful mineralized structures [13]. They are essential tools for upcoming advancements in the industrial, medical, and environmental domains due to their mechanical qualities, adjustable surface chemistry, biological advantages, and sustainable production. Titanium dioxide (TiO_2) nanofibers' strong surface reactivity has sparked a lot of interest in biomineralization research. The abundance of hydroxyl groups (-OH) on the surface of TiO_2 nanofibers makes it simple for them to draw in and hold onto calcium and phosphate ions from the surrounding biological fluids [14]. Consequently, hydroxyapatite (HA), the primary mineral present in bone and teeth, is stimulated to nucleate and grow [15]. TiO_2 nanofibers have frequently shown a strong apatite-forming capability in simulated body fluid (SBF) testing, a common method to assess biomineralization ability [16]. The mineralized TiO_2 nanofibers show their applicability for bioactive scaffolds and implants as they can closely mimic the composition and structure of real bone mineral [17]. Similarly, systems with enhanced mechanical properties, enhanced bioactivity, and tailored degradation rates that align with tissue healing processes

can be created by doping hybrid nanofiber systems with elements like silver, magnesium, or zinc [18].

Traditional TiO_2 nanofibers are generally brittle, which restricts their integration into soft, dynamic biological environments, despite the fact that they are biocompatible and structurally supportive [19]. Their mechanical mismatch may make it more difficult for cells to adhere, proliferate, and mineralize as a whole. On the other hand, the Flexible TiO_2 nanofibers form the structural backbone ('shish') for radially grown nanohydroxyapatite ('kebabs'), creating a biomimetic bone-mimicking architecture. These flexible scaffolds provide exceptional surface area and biocompatibility while maintaining mechanical resilience. Their compliant nature enables conformal tissue contact and adaptation to complex anatomical geometries, significantly improving cell adhesion and mineralization efficiency The nanofibrous substrate promotes uniform hydroxyapatite nucleation [4], with the resulting shish-kebab structure enhancing both mechanical strength and biological activity. This innovative design combines the durability of TiO_2 with the osteoconductivity of nHA, offering scalable production potential for advanced bone regeneration, dental repair, and orthopedic implant applications that require synergistic integration of synthetic and biological properties[20]. To sum up, flexible inorganic TiO_2 nanofibers are an important development that combines mechanical versatility with the superior chemical stability and photocatalytic qualities of TiO_2. They are therefore extremely important for sophisticated biomineralization applications, such as dental restoration, bone tissue engineering, and the creation of bioinspired materials.

This study examines the methods for creating flexible TiO_2 nanofibers, the processes influencing their biomineralization behavior, and the new uses for these nanofibers in biomedical domains. Additionally, the link between mineralization efficiency, surface chemistry, and fiber morphology is critically analyzed. In order to emphasize the important role that flexible TiO_2 nanofibers play in developing the next generation of biomineralized medical devices and tissue engineering, this work will focus on the interaction between material design and biological performance.

Materials and Methods

Polyvinyl pyrrolidone (PVP) with an average molecular weight of 360,000, titanium (IV) isopropoxide (97% purity), potassium dichromate (99%), sodium sulfide (95%), and zirconium (IV) acetate (99%) were obtained from Sigma-Aldrich, USA. Acetic acid (99.8%), cadmium nitrate tetrahydrate (99%), and ethanol (99.9%) were sourced from Shanghai Aladdin Biochemical Technology. All reagents were used without further purification.

Physicochemical Characterization

The morphology and microstructure of the fibrous membranes before and after biomineralization were characterized using scanning electron microscopy (SEM: Zeiss, Merlin Compact, Germany) equipped with energy-dispersive X-ray spectroscopy (EDS: IE250X-Max50, Oxford, UK). The internal architecture of the fibers was further investigated via transmission electron microscopy (TEM, Tecnai G2F20 S-Twin, operating at 200 kV). Crystalline phases of the samples were identified using X-ray diffraction (XRD: Ultima IV, Rigaku Co., Ltd., Japan) with Cu Kα radiation (λ = 1.5406 Å. Fourier transform infrared (FTIR) spectroscopy was conducted in the range of 500 cm^{-1} to 4000 cm^{-1} using a NICOLET 5700 instrument (Thermo Fisher Scientific, USA).

Fabrication of Flexible TiO_2 Nanofibrous Membrane

The flexible TiO_2 nanofiber membrane was fabricated as per our previous work [21]. In summary, a 5% by weight PVP solution was prepared using absolute ethanol. Separately, the titanium precursor was formulated by dissolving 4.8 g of titanium (IV) isopropoxide in

4 g of ethanol and 2.8 g of glacial acetic acid. Equal parts of the polymer and precursor solutions were combined and stirred for 1 hour. Subsequently, 0.27 g of zirconium (IV) acetate was added to the mixture, which was then stirred in an ice bath at 1000 rpm for 3 hours to yield a viscous electrospinning solution. This solution was loaded into a 5 ml syringe and electrospun using a Nano E-Spin setup at an applied voltage of 18 kV, with a flow rate of 1.5 ml/h and a tip-to-collector distance of 12 cm. The resulting fibers were subjected to calcination in a muffle furnace at 600°C, with a heating rate of 1°C per minute for 6 hours.

In Vitro Biomineralization Test

The biomineralization behavior of flexible TiO_2 nanofibrous membranes (NFMs) was evaluated using a simulated body fluid (SBF) solution as per the previous study with slight modification [22]. Briefly, the SBF was prepared by dissolving Hank's balanced salt, along with specific quantities of $MgSO_4$ (0.350 g), $NaHCO_3$ (0.185 g), and $CaCl_2$ (0.097 g), in 1 liter of distilled water. The pH of the solution was adjusted to 7.4, then filtered and stored for experimental use. The TiO_2 nanofiber membranes were immersed in equal volumes of the prepared SBF and incubated at 37 °C to mimic physiological conditions. The SBF solution was replaced every two days to maintain ionic stability. After incubation periods of 3, 7, and 14 days, the membranes were retrieved, thoroughly rinsed with deionized water, and subsequently freeze-dried. The dried samples were then subjected to detailed characterization using field-emission scanning electron microscopy (FE- SEM), X-ray diffraction (XRD), and Fourier-transform infrared spectroscopy (FTIR) to analyze the extent and nature of mineral deposition.

Results and Discussion

Flexibility of Prepared Nanofibrous Material

The incorporation of Zr notably affected the mechanical flexibility of electrospun TiO_2 nanofibers. As shown in Fig. 1(a), the Zr-doped TiO_2 mats exhibited enhanced flexibility, maintaining structural integrity under repeated bending without noticeable damage or fractures. This improvement is linked to the structural and crystallographic changes induced by Zr addition. Fig. 1(b) demonstrates the robust mechanical performance and effective load distribution properties of the Zr-doped TiO_2 nanofiber mat, suggesting its potential suitability for high-performance adhesive or interface-related applications.

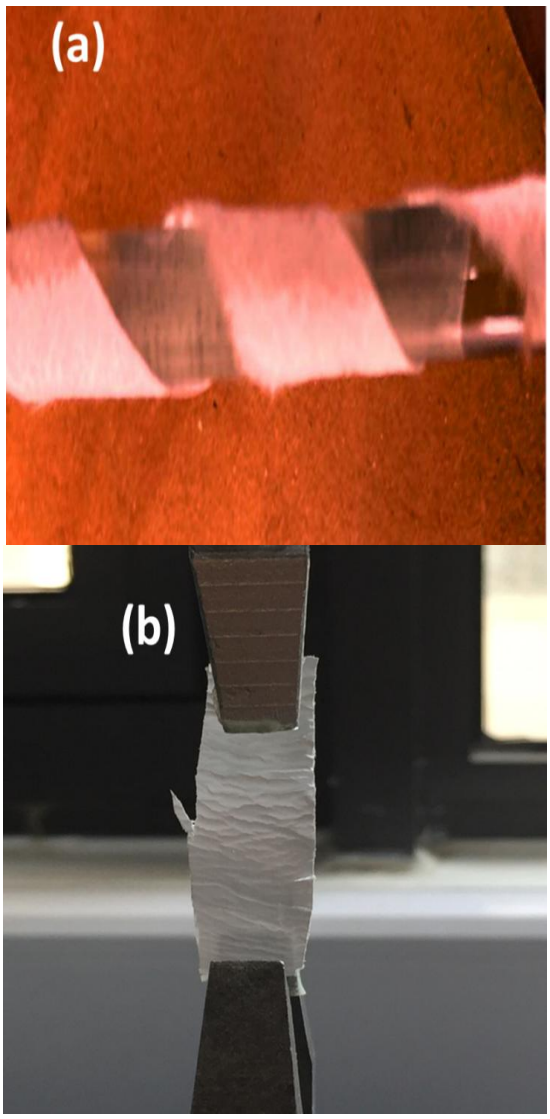

Figure 1: (a) Bending of TiO_2 NFM (b) Fatigue test of TiO_2 NFM under tensile load

Morphology Analysis

Scanning Electron Microscopy (SEM) was employed to analyze the morphological characteristics of TiO_2 nanofibrous membranes before and after biomineralization. Prior to biomineralization, the TiO_2 nanofibrous membranes exhibited smooth morphological features, as evident in the SEM images depicted in Fig.2 (a). These membranes formed a nonwoven mat composed of uniform, smooth, and continuous fibers. The fibrous network demonstrated high porosity and interconnectivity features critical for applications requiring a large surface area, such as tissue engineering, filtration, and catalysis. In post-biomineralization, significant morphological changes were observed on the surfaces of the TiO_2 nanofibers as shown in Fig. 2 (b-d). SEM images that nanohydroxyapatite grows radially outward from flexible TiO_2 nanofiber cores, generating a biomimetic shish-kebab morphology designed to replicate bone structure. The increased surface roughness and the emergence of granular features is the indicative of mineral deposition. A comparative analysis across samples subjected to different biomineralization durations showed a progressive increase in mineral deposition over time. Specifically, samples exposed to longer biomineralization periods exhibited denser and more extensive mineral coverage, as observed in the corresponding SEM images. EDS analysis as depicted in Table 1 also verifies the existence of calcium (Ca) and phosphorus (P), with Ca/P ratios nearing the typical value found in natural hydroxyapatite (approximately 1.64) for sample biomineralized for 14 days. This temporal trend highlights the dynamic nature of the biomineralization process and its pronounced influence on the structural attributes of TiO_2 nanofibrous membranes.

The TEM image of the Zr-doped TiO_2 nanofibers following biomineralization reveals key morphological attributes and surface modifications. At a magnification of 11,000×, the fibers retain their elongated, rod-like architecture, suggesting that the overall structural framework remains intact after the biomineralization process as depicted in Fig.3 (a). The fibrous network remains continuous and stable, indicating good morphological preservation under simulated biological conditions. Surface examination showed an increase in roughness and irregularity, which is attributed to the formation of a biomineral coating. This layer, likely composed of calcium phosphate deposits formed during exposure to simulated body fluid (SBF), resembles the mineral content of bone and plays a critical role in enhancing the material's bioactivity [23]. The presence of granular features on the fiber surface implies heterogeneous nucleation and growth of apatite-like minerals, validating the success of the biomineralization process. Additionally, contrast variations in the TEM image indicate a dense, crystalline core corresponding to the Zr-doped TiO_2 structure, surrounded by a less dense peripheral layer, representing the mineralized coating. Importantly, the fibers do not exhibit noticeable aggregation or collapse, demonstrating their mechanical robustness and chemical stability throughout the mineralization treatment. Complementary Energy-Dispersive X-ray Spectroscopy (EDS) analysis as depicted in Fig. 3 (b) supports these findings, with a distinct peak at ~0.52 keV indicating the presence of oxygen, and additional peaks near 3.69 keV (Kα) and 4.01 keV (Kβ) corresponding to calcium. A peak at approximately 2.01 keV (Kα) confirms the incorporation of phosphate groups, collectively validating the successful formation of a calcium phosphate layer on the nanofiber surfaces[24, 25].

X- Ray Diffraction (XRD) Analysis

The structural alterations on TiO_2 nanofibers induced by the biomineralization process were examined using X-ray diffraction (XRD) analysis as shown in Fig.4. The diffraction pattern of the pure TiO_2 nanofibers displayed prominent and well-defined peaks at 2θ values of 25.3° (101), 37.8° (004), 48.1° (200), and 62.8° (204), corresponding to the anatase phase of

TiO_2 [26, 27].

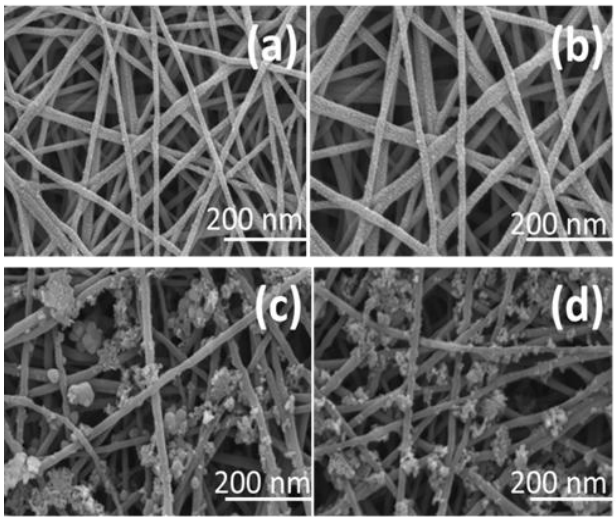

Figure 2: SEM images of (a) flexible TiO_2 NFM and (b- d) biomineralized flexible TiO_2 NFM after (b) 3 days (c) 7 days and (d) 14 days

Table 1 EDS data for TiO_2 nanofibrous membrane before and after biomineralization

Elements (at %)	O	Ti	Zr	Ca	P
Before Biomeneralization	64.2	29.2	0.5	0	0
After 14 days Biomeneralization	66.86	18.32	0.31	9.02	5.49

These findings confirm the presence of highly crystalline anatase TiO_2 nanofibers, which are well known for their photocatalytic activity and suitability for biological applications. After biomineralization the XRD pattern revealed significant changes in the crystalline structure of the TiO_2 nanofibers. New diffraction peaks appeared at 2θ values of 28.5°, 31.7°, and 66.3°, which were absent in the pure TiO_2 sample. The emergence of these peaks, along with a relative decrease in the intensity of the anatase TiO_2 peaks, indicates the formation of a new crystalline phase on the nanofiber surface during biomineralization. The peak at 31.7° (211) is attributed to hydroxyapatite ($Ca_{10}(PO_4)_6(OH)_2$) [28], a crucial mineral component of natural bone, while the peak at 28.5° (210) corresponds to a plane associated with calcium phosphate-based biominerals [29]. The peak observed at 66.3° is consistent with reflections characteristic of hydroxyapatite or related calcium phosphate phases, further supporting the formation of a crystalline calcium phosphate layer [30].

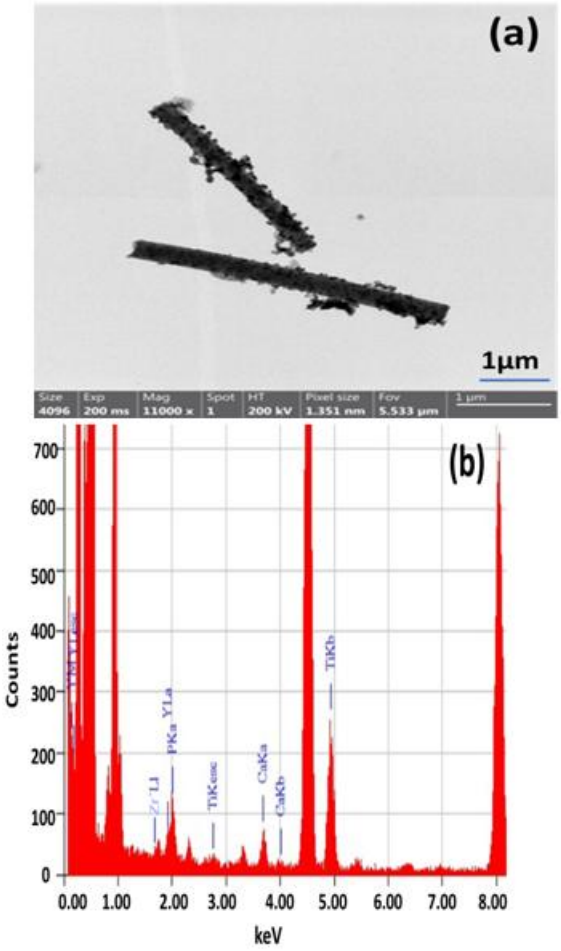

Figure 3: (a) TEM images of flexible TiO_2 NFM after 14 days of biomineralization and (b) EDS analysis of NFM after 14 days of biomineralization.

These structural transformations confirm the successful deposition of mineral phases, particularly hydroxyapatite, on the TiO_2 nanofibers, which is advantageous for applications in bone tissue engineering and related biomedical fields. The concurrent presence of nHA diffraction peaks with TiO_2 signals in XRD confirms the shish-kebab structure, evidencing crystalline HA 'kebabs' on TiO_2 nanofiber 'shish'. Correlated with SEM's periodic mineralization patterns, this demonstrates TiO_2's role as a nucleation scaffold for bone-mimetic HA organization, replicating native bone's mineralized collagen hierarchy.

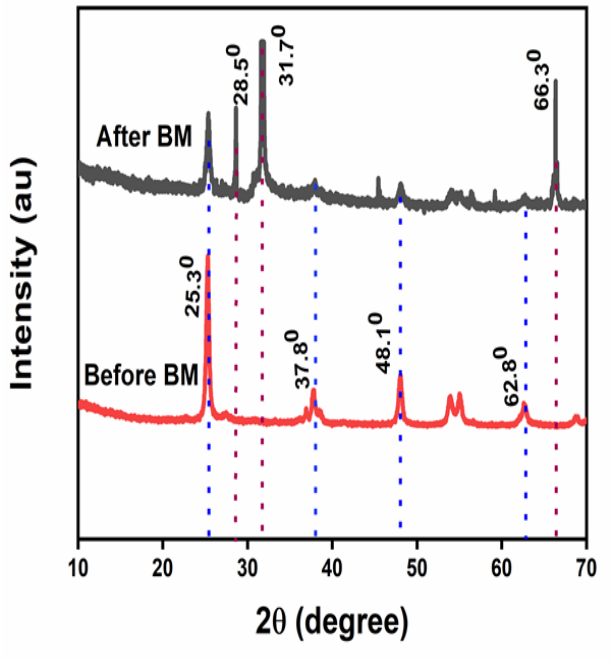

Figure 4: XRD pattern of flexible TiO_2 NFM before and after biomineralization

Fourier Transform Infrared Spectroscopy (FTIR) Analysis

TiO_2 nanofibers' surface chemistry alterations before and after biomineralization were characterized using Fourier-transform infrared spectroscopy (FTIR) as depicted in Fig.5. The non biomineralized TiO_2 sample showed distinctive peaks at 1625 cm^{-1}, 2325.01 cm^{-1}, and 2922.70 cm^{-1}. C–H stretching vibrations from adventitious hydrocarbons are responsible for the peak at 2922.70 cm^{-1} [31], whereas adsorbed CO_2 molecules may be the source of the peak at 2325.01 cm^{-1} [32].The peak at 1625 cm^{-1} indicates the presence of surface hydroxyl groups which is caused by the bending vibrations of physically adsorbed water molecules on the TiO_2 surface [33]. After biomineralization, the FTIR spectra showed notable alterations. The O–H stretching vibrations of hydroxyl groups and bound water were identified by a large and strengthened peak at 3418 cm^{-1}, which suggests increased hydrophilicity following mineral deposition. The non biomineralized TiO_2 sample did not have the new, distinct peaks that emerged at 1625.96 cm^{-1}, 1394.55 cm^{-1}, and 1034.65 cm^{-1}. A calcium phosphate phase, such as hydroxyapatite, is confirmed to be present on the TiO_2 surface by the peaks at 1394.55 cm^{-1} and 1034.65 cm^{-1}, which are attributed to the vibrational modes of phosphate groups (PO_4^{3-}) [34]. The peak at 1625.96 cm^{-1} suggests improved water adsorption [35]. The sharper peak observed at 3443cm^{-1} in biomineralized flexible TiO_2 is attributed to vibration of hydroxyl groups indicating a higher degree of hydroxylation and more uniform hydrogen bonding network on the surface. Overall, the FTIR analysis showed that the TiO_2 nanofibers have successfully undergone biomineralization, resulting in the development of mineral layers containing phosphate and increased surface hydroxylation. These outcomes are advantageous for enhancing biological interactions in biomedical applications.

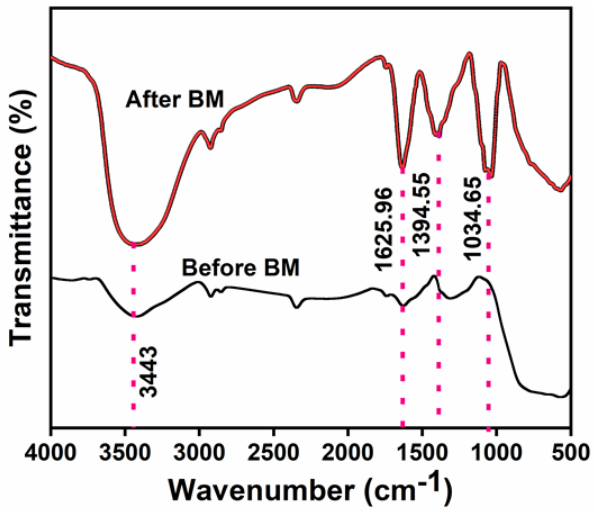

Figure 5: FTIR pattern of flexible TiO_2 NFM before and after biomineralization

Conclusions

The in vitro biomineralization analysis of TiO_2 nanofibrous membranes highlights their significant promise as bioactive scaffolds for bone tissue regeneration. Due to their flexible structure and high surface area, these nanofibers offer an ideal environment for the nucleation and growth of apatite crystals when immersed in simulated body fluid (SBF), replicating the early stages of bone mineral formation. Advanced characterization techniques such as scanning electron microscopy (SEM), energy-dispersive X-ray spectroscopy (EDS), and X-ray diffraction

(XRD), Fourier transform infrared spectroscopy (FTIR), confirmed the presence of calcium phosphate layers on the fiber surfaces. Notably, the Ca/P ratio detected through EDS closely approximates that of natural hydroxyapatite, suggesting that the mineral phase formed is chemically similar to bone tissue.

Furthermore, the nanofibrous morphology of the TiO_2 membranes closely resembles the native extracellular matrix (ECM), providing not only structural support but also enhancing cellular interactions and biological responses necessary for bone integration. The successful formation of apatite under physiological-like conditions demonstrates the material's inherent bioactivity and its suitability for use in bone repair applications. In addition to their mineralization capability, the mechanical flexibility and conformability of these membranes enable them to adapt to complex anatomical shapes, making them suitable for various clinical scenarios.

Protein adsorption on biomaterials in vitro frequently differs from physiological conditions, critically affecting cellular interactions. This discrepancy is particularly evident in bone research, where standard SBF solutions omit essential osteogenic proteins (BMPs, collagen) present in vivo. Such protein-deficient environments may generate misleading mineralization outcomes that poorly correlate with natural bone development processes. To maximize their effectiveness, further research should explore in vivo performance, degradation rates over time, and surface or compositional modifications aimed at enhancing their biological functionality. Such studies are essential to advancing these membranes toward real-world applications in orthopedic and dental tissue engineering.

Acknowledgements

We sincerely thank Liaocheng University, China, for assisting with laboratory facilities and sample characterization. We are equally grateful to the Indian Institute of Technology, Hyderabad, India, and the Department of Pharmacy Maharajgunj Medical Campus, Tribhuvan University, Nepal, for providing essential laboratory support. Their support played a vital role in making this study possible.

Author's contribution statement

S. Pandeya: Methodology, Investigation, Formal analysis, Writing: original draft, **S. K. Sah**: Formal analysis, Investigation **Z. Li:** Supervision, Visualization, editing, **M. K. Joshi:** Conceptualization, Formal analysis, Writing-review &editing, Supervision.

Conflict of Interest

The authors do not have any conflict of interest related to this research work.

Data Availability Statement

The data supporting the findings of this study are available from the corresponding authors upon reasonable request.

References

1. Y. Zhou, K. Liu, and H. Zhang, Biomimetic mineralization: From microscopic to macroscopic materials and their biomedical applications, *ACS Applied Bio Materials,* 2023, 6 (9), 3516-3531 https://doi.org/10.1021/acsabm.3c00109
2. L. Suamte, A. Tirkey, J. Barman, and P. Jayasekhar Babu, Various manufacturing methods and ideal properties of scaffolds for tissue engineering applications, *Smart Materials in Manufacturing,* 2023 , 1, 100011. 10.1016 /j.smmf.2022.100011
3. Z. Xu, M. Wu, Q. Ye, D. Chen, K. Liu, and H. Bai, Spinning from nature: Engineered preparation and application of high-performance bio-based fiber, *Engineering,* 2022, 14, 100-112. https: // doi.org / 10.1016/j.eng.2021.06.030
4. E. Campodoni, T. Patricio, M. Montesi, A. Tampieri, M. Sandri, and S. Sprio, Biomineralization process generating hybrid nano- and micro-carriers, *Core-Shell Nanostructures for Drug Delivery and Theranostics*, M. L. Focarete and A. Tampieri, Eds., ed: Woodhead Publishing, 2018, 19-42.

https:// doi.org /10.1016/B978-0-08-102198-9.00003-X

5. E. Campodoni, M. Montanari, C. Artusi, G. Bassi, F. Furlani, M. Montesi, *et al.*, Calcium-based biomineralization: A smart approach for the design of novel multifunctional hybrid Materials, *Journal of Composites Science,* 2021, 5 (10), 278 https://doi.org/10.3390/jcs5100278
6. Y. Chen, F. Yanmin, J. Deveaux, M. Masoud, F. Chandra, H. Chen, *et al.*, Biomineralization forming process and bio-inspired nanomaterials for biomedical application, *A review, Minerals,* 2019, 9 (2), 68 . https: // doi.org / 10.3390/ min9020068
7. Kenry and C. T. Lim, Nanofiber technology: current status and emerging developments, *Progress in Polymer Science,* 2017, 70, 1-17..https://doi.org / 10.1016/j.progpolymsci.2017.03.002
8. X. Zhan, Z. Wen, X. Chen, Q. Lei, Y. Chen, L. Zhou, *et al.*, Polyphenol-mediated biomimetic mineralization of sacrificial metal-organic framework nanoparticles for wound healing, *Cell Reports Physical Science,* 2022, 3 (11), 101103. https://doi.org /10.1016/ j.xcrp.2022.101103
9. S. H. Kim, M.-R. Ki, Y. Han, and S. P. Pack, Biomineral-based composite materials in regenerative medicine, *International Journal of Molecular Sciences,* 2024 ,25 (11), 6147. https://doi.org/10.3390/ijms25116147
10. M.H. Hong, J. H. Lee, H. S. Jung, H. Shin, and H. Shin, Biomineralization of bone tissue: calcium phosphate-based inorganics in collagen fibrillar organic matrices, *Biomaterials Research,* 2022 26(1),42. https://doi.org/10.1186/s40824-022-00288-0
11. Y. Zhang, X. Hu, Y. Wang, and N. Jiang, A critical review of biomineralization in environmental geotechnics: Applications, trends, and perspectives, *Biogeotechnics,* 2023, 3(2), 100177. 10.1016/ j.bgtech.2023.100003
12. K. Qin, Z. Zheng, J. Wang, H. Pan, and R. Tang, Biomineralization strategy: from material manufacturing to biological regulation, *Giant,* 2024 ,19, 100317. 10.1016/ j.giant.2024. 100317
13. H. Omidian and E. J. Gill, Nanofibrous scaffolds in biomedicine, *Journal of Composites Science,* 2024, 8 (7), 269 . https://doi.org/10.3390/jcs8070269
14. J. Wang, L. Xiaonao, R. Li, P. Qiao, L. Xiao, and J. Fan, TiO_2 nanoparticles with increased surface hydroxyl groups and their improved photocatalytic activity, *Catalysis Communi-cations,* 2012, 19, 96–99.
15. J. Park, B. J. Kim, J. Y. Hwang, Y. W. Yoon, H. S. Cho, D. H. Kim, *et al.*, In-vitro mechanical performance study of biodegradable polylactic acid/ hydroxyapatite nanocomposites for fixation medical devices, *J Nanosci Nanotechnol,* 2018 , 18 (2), 837-841. 10.1016 / j.catcom. 2011. 12. 028
16. A. Kodama, S. Bauer, A. Komatsu, H. Asoh, S. Ono, and p. Schmuki, Bioactivation of titanium surfaces using coatings of TiO_2 nanotubes rapidly re-loaded with synthetic hydroxyapetite, *Acta biomaterialia*, 2009, 5, 2322-30 10.1016/j.actbio. 2009.02.032
17. S. Jiang, M. Wang, and J. He. A review of biomimetic scaffolds for bone regeneration, *Cell-Free Strategy*, 2020, 6 (2), 10206. https://doi.org/10.1002/btm2.10206
18. S. Mondal, S. Park, J. Choi, T. T. H. Vu, V. H. M. Doan, T. T. Vo, *et al.*, Hydroxyapatite: A journey from biomaterials to advanced functional materials, *Advances in Colloid and Interface Science,* 2023, 321, 103013. https://doi.org/10.1016/j.cis.2023.103013
19. A. R. Borah, P. Hazarika, R. Duarah, R. Goswami, and S. Hazarika, Biodegradable electrospun membranes for sustainable industrial applications, *ACS Omega,* 2024, 9 (10), 11129-11147. https://doi.org/10.1021/acsomea. 3c09564
20. D. Gugulothu, A. Barhoum, R. Nerella, R. Ajmer, and M. Bechelany, Fabrication of nanofibers: electrospinning and non-electrospinning techniques, *Handbook of Nanofibers*, 2019,

45-77. https: // doi.org/10.1007/978-3-319-53655-2_6

21. S. Pandeya, R. Ding, Q. Shang, X. Zhu, Y. Ma, X. Han, *et al.*, A flexible Ag_2S QD sensitized TiO_2 Janus photocatalytic nanofiber membrane for visible light organic pollutant degradation and COD removal, *Colloids and Surfaces A: Physicochemical and Engineering Aspects,* 2025 , 707, 135946. 10.1016/j.colsurfa.2024.135946
22. B. Maharjan, J. Park, V. K. Kaliannagounder, G. P. Awasthi, M. K. Joshi, C. H. Park, *et al.*, Regenerated cellulose nanofiber reinforced chitosan hydrogel scaffolds for bone tissue engineering, *Carbohydrate Polymers 2021,* 251, 117023. 10.1016/j.carbpol.2020.117023
23. F. Baino and S. Yamaguchi. The use of simulated body fluid (SBF) for assessing materials bioactivity in the context of tissue engineering: review and challenges, *Biomimetics,*2020, 5 (4)57. 10.3390/biomimetics5040057
24. L. J. Hicks. X-ray spectroscopy and electron microscopy of planetary materials, University of Leicester, 2015.
25. W. Vanderlinde, Energy dispersive X-ray analysis, *Microelectronics Failure Analysis: Desk Reference*, ed: ASM International, 2019, 434-446. 10.31399/ asm.tb. mfadr7. t91110434
26. S. Shanmugam, B. Madheswaran, and T. Soga, Synthesis of titanium dioxide nanoparticles with desired ratio of anatase and rutile phases and the effect of high temperature annealing, *Transactions of the Materials Research Society of Japan,* 2018, 43 (5), 255-261. https: //doi.org/10.14723/tmrsj.43.255
27. V. Paramasivam, R. K. Beemaraj, M. Sundaram, and A. Prasath, Investigate the characterization and synthesis process of Titanium dioxide nanoparticles, *Materials Today: Proceedings,* 2022 , 52 (3), 1140-1142. https://doi.org/10.1016/j.matpr.2021.11.009
28. R. P. Singh, J. P. Singh, C. Singh, T. Kaur, and A. Pal, Synthesis, characterization and in-vitro bioactivity evaluation of mesoporous $Ca_{10-x}Fe_x(PO_4)_6(OH)_2$ nanorods-like particles, *Ceramics International,* 2020, 46 (8) , 12156 - 12164.
29. M. Furko, Z. E. Horváth, O. Czömpöly, K. Balázsi, and C. Balázsi, Biominerals added bioresorbable calcium phosphate loaded biopolymer composites, *International Journal of Molecular Sciences,* 2022, 23 (24), 15737, 2022. https://doi.org/10.3390/ijms232415737
30. M. Merle, J. Soulié, C. Sassoye, P. Roblin, C. Rey, C. Bonhomme, *et al.*, Pyrophosphate-stabilised amorphous calcium carbonate for bone substitution: toward a doping-dependent cluster-based model, *Cryst Eng Comm,* 2022, 24(45), 8011-8026. shttps://doi.org/10.1039/D2CE00936F
31. L. Mino, A. Zecchina, G. Martra, A. M. Rossi, and G. Spoto, A surface science approach to TiO_2 P25 photocatalysis: An in situ FTIR study of phenol photodegradation at controlled water coverages from sub-monolayer to multilayer, *Applied Catalysis B: Environmental,* 2016, 196, 135-141. https://doi.org/10.1016/j.apcatb.2016.05.029
32. L. Mino, G. Spoto, and A. M. Ferrari, CO_2 capture by TiO_2 anatase surfaces: a combined DFT and FTIR study, *The Journal of Physical Chemistry C,* 2014, 118 (43), 25016-25026. https://doi.org/ 10.1021/jp507443k
33. A. León, P. Reuquen, C. Garín, R. Segura, P. Vargas, P. Zapata, *et al.*, FTIR and Raman characterization of TiO_2 nanoparticles coated with polyethylene glycol as carrier for 2-methoxyestradiol, *Applied Sciences,* 2017, 7(1), 49. https://doi.org/ 10. 3390 / app 7010049
34. I. Erceg, A. Selmani, A. Gajović, I. Panžić, D. Iveković, F. Faraguna, *et al.*, Calcium phosphate formation on TiO_2 nanomaterials of different dimensionality, *Colloids and Surfaces A: Physicochemical and Engineering Aspects,*2020, 593, 124615, 2020. 10.1016/ j.colsurfa.2020 .124615
35. E. Campodoni, M. Montanari, C. Artusi, L. Bergamini, G. Bassi, E. Destro, *et al.*,

Biomineralization: A new tool for developing eco-sustainable Ti-doped hydroxyapatite-based hybrid UV filters, *Biomaterials Advances*, 2023, 151, 21347.
https: // doi.org /10.1016 / j.bioadv. 2023.213474